

Diagnosis of Periodontal Disease from Saliva Samples Using Fourier Transform Infrared Microscopy Coupled with Partial Least Squares Discriminant Analysis

Satoshi FUJII,^{*1,*2} Shinobu SATO,^{*2,*3} Keisuke FUKUDA,^{*2} Toshinori OKINAGA,^{*4} Wataru ARIYOSHI,^{*4} Michihiko USUI,^{*5} Keisuke NAKASHIMA,^{*5} Tatsuji NISHIHARA,^{*4} and Shigeori TAKENAKA^{*2,*3†}

^{*1} Department of Bioscience and Bioinformatics, Kyushu Institute of Technology, Iizuka, Fukuoka 820-8502, Japan

^{*2} Research Center for Bio-microsensing Technology, Kyushu Institute of Technology, 1-1 Sensui-cho, Tobata, Kitakyushu, Fukuoka 804-8550, Japan

^{*3} Department of Applied Chemistry, Kyushu Institute of Technology, 1-1 Sensui-cho, Tobata, Kitakyushu, Fukuoka 804-8550, Japan

^{*4} Division of Periodontology, Department of Oral Function, Kyushu Dental University, Department of Oral Function, Kokura-kita, Kitakyushu, Fukuoka 803-8580, Japan

^{*5} Division of Infections and Molecular Biology, Department of Health Promotion, Kyushu Dental University, 2-6-1 Manazuru, Kokura-kita, Kitakyushu, Fukuoka 803-8580, Japan

Diagnosis of periodontal disease by Fourier transform infrared (FT-IR) microscopic technique was achieved for saliva samples. Twenty-two saliva samples, collected from 10 patients with periodontal disease and 12 normal volunteers, were pre-processed and analyzed by FT-IR microscopy. We found that the periodontal samples showed a larger raw IR spectrum than the control samples. In addition, the shape of the second derivative spectrum was clearly different between the periodontal and control samples. Furthermore, the amount of saliva content and the mixture ratio were different between the two samples. Partial least squares discriminant analysis was used for the discrimination of periodontal samples based on the second derivative spectrum. The leave-one-out cross-validation discrimination accuracy was 94.3%. Thus, these results show that periodontal disease may be diagnosed by analyzing saliva samples with FT-IR microscopy.

Keywords Periodontal disease, Fourier transform infrared (FT-IR) microscopy, partial least squares (PLS) discriminant analysis, leave-one-out cross-validation (LOOCV)

(Received August 31, 2015; Accepted October 17, 2015; Published February 10, 2016)

Introduction

Periodontal diseases refer to a group of diseases affecting the periodontium, which includes the gingiva, periodontal ligament, and alveolar bone. Periodontal disease commonly causes swelling and bleeding of the gingiva, and severe progression of the disease may lead to loss of attachment of the tooth. For prevention and treatment of periodontal disease, it is important to identify periodontal disease in the early to moderate stages. Therefore, a simple and quick diagnostic technique is required to evaluate periodontal disease during mass examinations.

Periodontal disease is currently diagnosed by using the following traditional clinical assessments: probing pocket depth (PPD), bleeding on probing (BOP), probing attachment level (PAL), tooth mobility, and radiography. All these assessments involve clinical examinations by dentists, and therefore, they are somewhat subjective and time consuming. Although several microbial, biochemical, and genetic tests for disease diagnosis

have been developed, these tests are regarded as supplementary analysis and are not routinely used in clinical practice. Furthermore, periodontal disease is caused by several complex factors, making it challenging to diagnose by using only one of these practical tests. For example, most periodontal diseases are caused by pathogenic bacteria in the plaque; however, some gingival diseases are not induced by plaque formation. In addition, immune reactions against pathogens vary between individuals. Moreover, lifestyle and stress are some of the factors affecting the development of periodontal disease.¹⁻³ Therefore, monitoring of complex factors related to the oral condition of a patient is important for the diagnosis of periodontal disease.

Fourier transform infrared (FT-IR) microscopy is a technique used to analyze the chemical properties of a substance. It measures the amount of radiation absorbed by a sample when excited by infrared light. The IR spectrum obtained provides information regarding the functional groups of molecules and conformational properties of biological substances. It has an intrinsic shape because it represents chemical constituents such as proteins, lipids, and nucleic acids. The IR spectrum of a biological sample is formed by superposition of all infrared-

† To whom correspondence should be addressed.
E-mail: shige@che.kyutech.ac.jp

Table 1 Characteristics of saliva samples obtained from patients with periodontal disease

Sample ID	Lesion	Treatment stage
M	Established-Advanced	Undergoing scaling
N	Established-Advanced	Undergoing scaling
O	Advanced	Received scaling
P	Early-Established	First medical examination
Q	Established	Undergoing scaling
R	Established-Advanced	Undergoing scaling
S	Early-Established	First medical examination
T	Established-Advanced	First medical examination
U	Established	First medical examination
V	Established	First medical examination

active vibrational modes of all the molecules present in the sample. Therefore, FT-IR has been recently applied to analyze biological samples for the following purposes: classification of bacteria,⁴⁻¹¹ discrimination of cancer cells,¹²⁻²⁰ detection of scrapie,^{18,21-23} and histopathologic recognition.^{24,25} Importantly, Xiang *et al.* used mid-infrared spectroscopy to analyze the gingival crevicular fluid (GCF) in order to determine differences between periodontitis, gingivitis, and normal sites.²⁶

Whole saliva consists of a mixture of fluids such as water, proteins, and electrolytes secreted by the salivary glands; non-salivary components derived from the GCF; oral bacteria, including their enzymes and bacterial products; viruses and fungi; blood and serum cells, desquamated epithelial cells; and food debris.^{27,28} Therefore, it is thought that the saliva of patients with periodontal disease contains not only pathogenic bacteria and their products but also immunological proteins secreted during the biological response. Saliva samples can be easily collected from patients, and therefore, it can be assessed for the diagnosis of periodontal disease during early-stage clinical trials.

Therefore, in this study, to establish a method for the early diagnosis of periodontal disease, we used FT-IR microscopy to analyze saliva samples from patients with periodontal disease and healthy volunteers based on the differences in the constituents of the two samples. Partial least squares discriminant analysis (PLS-DA) was used for the discrimination of periodontal samples based on the second derivative spectrum.

Experimental

Sample preparation

We analyzed 22 saliva samples, which were collected from 12 healthy volunteers (A - L) and 10 patients with periodontal disease (M - V). In the patient group, the severity of periodontal disease ranged from slight illness to serious disease; moreover, the patients were in different stages of treatment (Table 1). Volunteers in the control group had no subjective symptoms of periodontal disease.

The saliva samples were collected according to the following protocol: (1) The subjects washed their mouths with tap water for 1 min, (2) they waited for 5 min, (3) they gargled with 15 mL of physiological saline for 1 min, and (4) they spat the saline into a Falcon tube. The saliva samples thus obtained were transferred to 1.0 mL microcentrifuge tubes (Eppendorf). The samples were centrifuged at 10000 rpm for 10 min, the supernatants were discarded, 1 mL of saline was added, and the tubes were vortexed for 1 min. This procedure was repeated

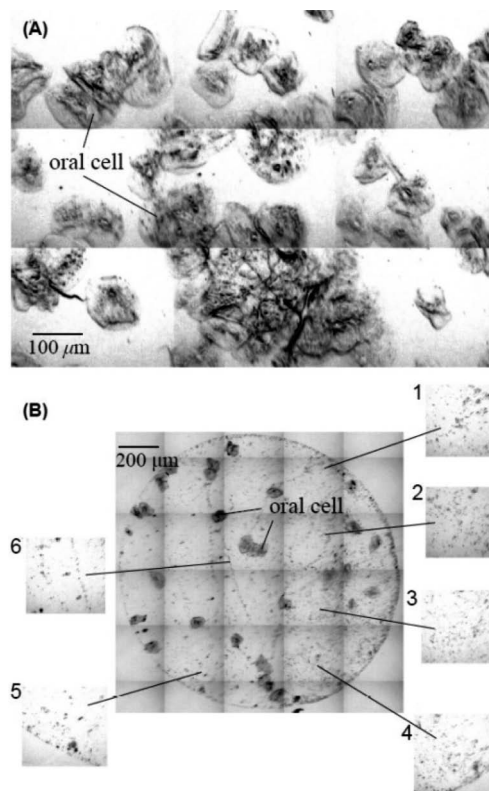


Fig. 1 (A) Photomicrograph of a saliva sample. The shaded portions indicate oral cells. (B) The pictures numbered 1 to 6 were some example areas that were manually selected to avoid oral cells.

twice. Next, the supernatants were removed, 50 μL of pure water was added, and the contents of the tube were vortex-mixed for 1 min. Finally, 1.0 μL of the supernatant was spotted, at an approximate diameter of 1.0 mm, on a calcium fluoride plate.

FT-IR analysis

FT-IR spectra of the samples were obtained using a Perkin-Elmer Spotlight 300 FT-IR imaging system. At first, samples were prepared for spectroscopic measurements by drying saliva samples to minimize spectral contributions from water vapor and carbon dioxide. Samples were put on CaF_2 plate and were put into the sample chamber of the spectrometer system. The sample chamber was purged with dry air for 1 h before FT-IR measurement. This FT-IR system was equipped with a computer-controlled x-y stage, which can measure arbitrary sites on the sample. In this study, IR spectra were measured with an aperture diameter of 200 μm at approximately 15 sites per sample, which were manually selected under the microscope to avoid oral cells (Fig. 1). This system was equipped with a liquid nitrogen-cooled MCT (Hg-Cd-Te) line detector. Transmission/absorption spectra were obtained from 4000 to 950 cm^{-1} , with a spectral resolution of 6 cm^{-1} and 256 scans per site at room temperature. All spectral data were converted into absorbance for further analysis.

IR data evaluation

The spectral data obtained were processed using R software.²⁹ The spectra were only used for wavelengths ranging from 2000 to 950 cm^{-1} . To correct baseline differences, monomial fitting to raw spectra with baseline suppression by polynomial fitting

was performed using the *baseline.modpolyfit* function in the baseline package for R.³⁰ Signal-to-noise (*S/N*) ratios were determined from the raw spectra (using the maximum value in the amide I region (1600 – 1700 cm⁻¹) minus the mean value in the 1800 – 1900 cm⁻¹ range as the signal and standard deviations in the 1800 – 1900 cm⁻¹ region as the noise). The data with *S/N* ratios less than 50 were discarded. Finally, the 6 – 12 data were retained for each sample. The second derivatives of raw IR spectra were calculated using a 9-point Savitzky-Golay algorithm. Vector normalization was carried out for the second derivatives.^{10,12,21,23,31,32}

IR data comparison

To compare the IR spectral data between the two groups, a two-way ANOVA of the log₂ signal ratios was performed, which were defined before, and cluster analysis was carried out for the normalized second derivatives. Two-way ANOVA indicated whether the variance in the log₂-signals was associated with periodontal disease or normal samples. To compare the shapes of the normalized second derivatives, cluster analysis was performed using normalized second derivatives between 2000 and 1012 cm⁻¹, which were averaged for each saliva sample. Spectral distances were calculated as the Euclidean distance, and Ward's algorithm was used for hierarchical clustering.

PLS-DA

Dimension reduction was performed to construct a regression model for the multicollinear spectrogram data. PLS-DA was performed for multivariate classification. The normalized second derivative spectra between 2000 and 1012 cm⁻¹ (165 points) from all sites of all the samples were used for the PLS-DA. PLS were calculated by using the *pls* function in the *pls* package of R.³³ The kernel PLS algorithm was applied for PLS.^{34,35} The latent vectors obtained by PLS were used as explanatory variables for regression. Value 1 for periodontal disease and 0 for control were used as *Y* (class membership, discriminant variable). The regression equation was as follows:

$$\hat{Y} = \beta_0 + \beta_1 T_1 \dots + \beta_{165} T_{165}$$

where \hat{Y} is the predicted *Y*, T_1 to T_{165} are the latent vectors obtained by PLS, β_1 to β_{165} are the regression coefficients, and β_0 the intercept. *Y* is categorical data represented by 0 and 1, but a normal Gaussian linear model was applied because of the differences in the stage of periodontal disease progression and intermediate symptoms. The threshold of \hat{Y} was set to 0.5, and the samples with $\hat{Y} > 0.5$ were discriminated as periodontal disease samples. The accuracy of the discrimination was calculated by leave-one-out cross-validation (LOOCV). In LOOCV, one dataset is used as the testing data, whereas the other dataset is used as the training dataset to estimate the validation data, and this procedure is repeated the number of the data times. In our study, data were obtained at several sites for each saliva sample. The data derived from one site of a sample were similar to the others in the sample, and so, the LOOCV estimated higher accuracy. Thus, when spectral data from a sample was used as the testing data, the other data from the sample were excluded from the training data. The number of latent vectors used for the regression model was determined in order to attain the highest accuracy of LOOCV.

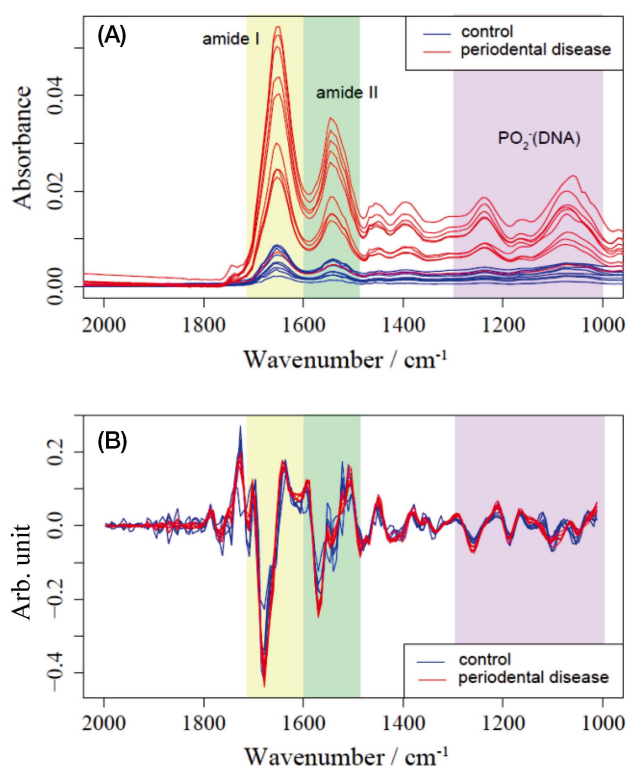


Fig. 2 (A) IR raw spectra and (B) its second derivative spectra from saliva samples. Each line represents a spectrogram, which was averaged from spectral data obtained from one spot of a sample. The red lines indicate periodontal disease samples, and the blue lines indicate control samples.

Results

IR spectra of the saliva samples

The average raw spectra of the control saliva samples (samples A – L) and periodontal disease samples (samples M – V) are shown in Fig. 2A, which were corrected baseline according to the range (1900 – 1000 cm⁻¹) and were averaged in spectra of 6 – 12 spots per sample. Figure 2B shows the average normalized second derivatives. These spectra showed some major absorbance ranges, which were important for discriminating cell components. The most distinctive peak was between 1800 and 1500 cm⁻¹, whose spectral features are dominated by the >C=O stretching absorption band of ester carbonyl (1738 cm⁻¹) and the amide band of proteins. The amide I band, which is mainly the amide >C=O stretching frequencies of the protein backbones, was observed between 1700 and 1600 cm⁻¹. Furthermore, the amide II band was observed, which is mainly shaped by coupled N-H bending and C-N stretching vibrations between 1600 and 1500 cm⁻¹. The regions between 1300 and 1000 cm⁻¹ represent characteristic absorbance bands, which are concerned with P=O double bond stretching modes of phosphate groups in the DNA/RNA backbone structure and in the teichoic and lipoteichoic acids present in the cell wall of gram-positive bacteria and with C-C stretching modes in the aromatic ring of carbohydrates. Moreover, the absorbance band between 1470 and 1350 cm⁻¹ is associated with >CH₂ stretching and bending vibrations, including the fatty acids of the cell membrane. Spectral peaks other than those mentioned above were not assigned precisely, but these peaks provided important chemical information

specific to a sample. Thus, the IR spectra of the saliva samples represented the complex of the absorbance bands derived from several biological components.

Raw IR spectra

The intensities of absorbance of the raw IR spectra in the periodontal disease samples were clearly larger than those of the control samples (Fig. 2A). Figure 3 shows the differences in the \log_2 -signal values of raw IR spectra, which were the maximum values between 1600 and 1700 cm^{-1} minus the mean value between 1800 and 1900 cm^{-1} , for each sample. The average of the \log_2 -signal values in the periodontal disease samples (average: -5.30) was larger than in the control samples (average: -7.50), but samples G, H, and I had larger values than the other samples from the control group, and sample S had a lower value than the others in the periodontal disease group.

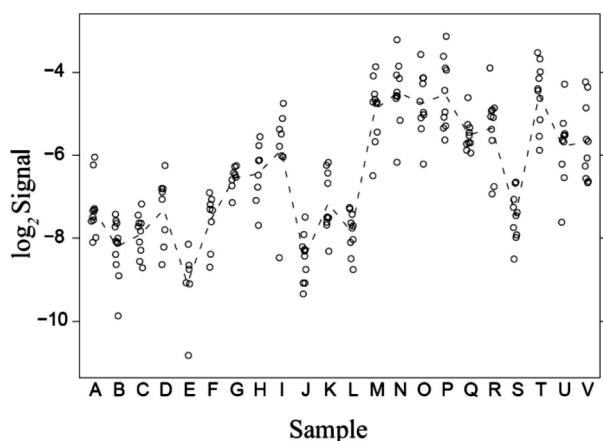


Fig. 3 The \log_2 -signal values of raw IR spectra (Fig. 2A), which were the maximum values between 1600 and 1700 cm^{-1} minus the mean value between 1800 and 1900 cm^{-1} . Each point represents the value of one measured spot. The dashed line represents the average value in each sample.

Both variances of \log_2 signal, whether in the periodontal disease or control samples, were significant by ANOVA (p -value $< 2.2 \times 10^{-16}$). The difference in \log_2 signals between periodontal disease and control samples was significantly large, but the difference between individual samples was also large.

Normalized second derivatives

The properties of the normalized second derivative spectrograms were different between the periodontal disease and control samples (Fig. 2B). Therefore, hierarchical cluster analysis was performed to compare the differences between the spectrograms. Dendrograms showing three distinct groups are shown in Fig. 4. Two periodontal disease samples, samples S and Q, were misclassified. The shapes of these spectra were similar to the shape of the controls.

PLS-DA

The score plot of the first three latent vectors for projection of data in the PLS space is shown in Fig. 5A. Two distinct groups were formed during the classification trial. Figure 5B shows the plot of the loadings of the latent vectors 1–3 of PLS. The contribution of the spectral region between 1700 and 1600 cm^{-1} , derived from amide I, appeared large on all three latent vectors.

The latent vectors from 1 to 5 of PLS were used for regression analysis. The predicted values \hat{Y} were plotted for each sample in Fig. 6. The values obtained for the periodontal disease samples were clearly larger than those obtained for the control samples. The variances in the samples were small, and most of the values did not overlap between the two study groups. The accuracy for the discrimination of periodontal disease by LOOCV was 94.3% using PLS regression, with the threshold of predicted values $\hat{Y} > 0.5$.

Discussion

Difference between the IR spectra of saliva samples obtained from patients with periodontal disease and control subjects. The results of this study showed that periodontal disease could be diagnosed by analyzing saliva samples using FT-IR microscopy.

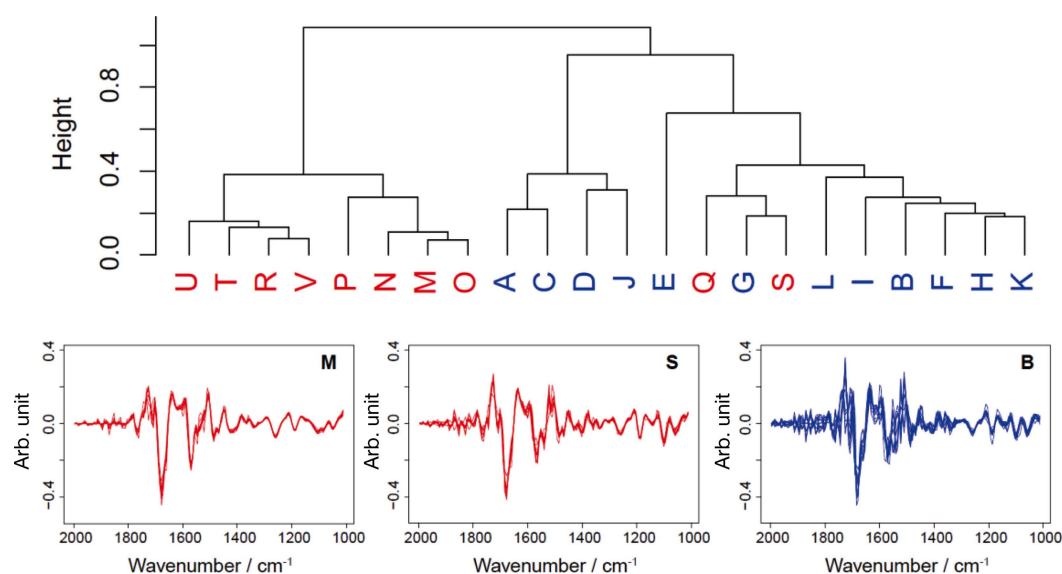


Fig. 4 Cluster analysis of normalized second derivative spectra of saliva samples. The dendrograms show spectra-periodontal disease (M), control (B), and misclassified spectra (S).

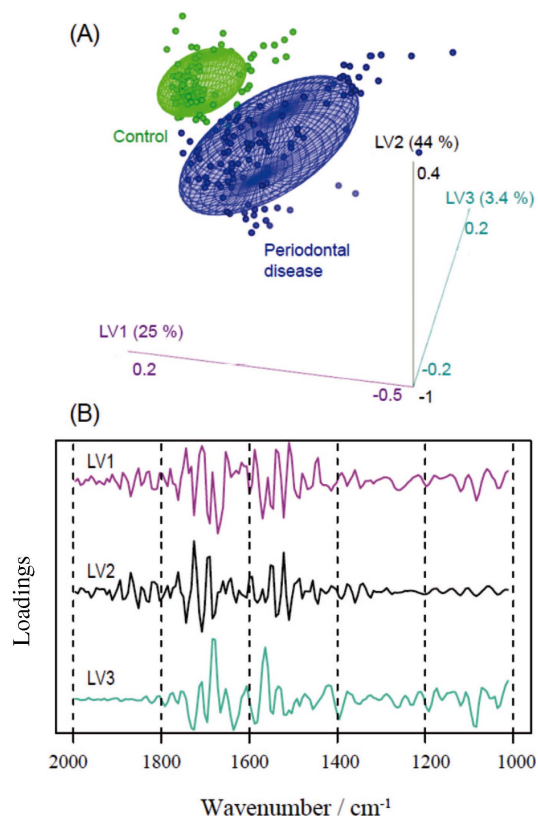


Fig. 5 (A) The PLS score plot and (B) the loadings from 2000 cm⁻¹ to 1000 cm⁻¹ showing the first three latent vectors.

The IR spectra of the saliva samples were formed because of accumulation of the absorbance bands of individual biomolecules. First, the differences in the absorbance on raw spectra reflected the differences in the quantities of the chemical components. The absorbance of periodontal disease samples was clearly larger over the thorough spectrum, although all saliva samples were collected by using the same protocol (Fig. 2A). Moreover, the log₂-signal values, which were the maximum value minus the baseline value, were also larger in the periodontal disease group (Fig. 3). If both quantity of the chemical components in saliva sample and control sample were equal, the intensities of the absorbance and log₂-signal should be also equal. But in this case, the absolute quantities of the chemical components are assumed to be larger in the periodontal disease samples than in the control samples. In other words, the density of any chemical component of the saliva collected from a patient with periodontal disease was higher than that of saliva collected from a control subject. Second, the differences in the shape of the normalized second derivatives reflected the mixture ratio of several components. Thus, the shape of the normalized second derivatives differed between periodontal disease samples and controls (Fig. 2B). The two distinct groups could be discriminated by cluster analysis using the normalized second derivatives except for S and Q (Fig. 4). The mixture ratio of the components in the saliva is assumed to differ between periodontal disease and control samples. Thus, the properties of the saliva in patients with periodontal disease appear to differ from the normal condition. In fact, it has been recognized that gram-negative bacteria such as *porphyromonas gingivalis*, *agggregatibacter actinomycetemcomitans*, and *prevotella intermedia* propagate in the pockets of the gingival sulcus in

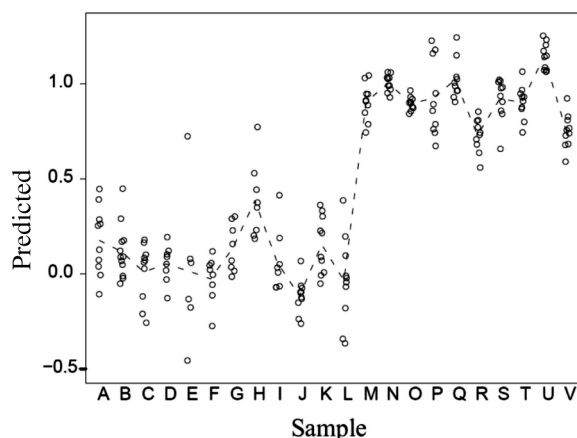


Fig. 6 The plot of predicted values by PLS-DA. The first four latent vectors were used for PLS regression. Values greater than 0.5 were discriminated as periodontal disease. Each open circle represents the value of one measured spot. The dashed line represents the average value in each sample.

patients with periodontal disease.^{2,36-38} Moreover, several salivary components such as enzymes, immunoglobulins, proteins, hormones, and other small substances may be present in the saliva of patients with periodontal disease.^{2,28} Several biological constituents were present in larger quantities in the saliva samples of patients with periodontal diseases than in the control saliva samples, and the mixture ratios of the components were different. Thus, these quantitative differences in the components of the saliva samples were reflected as differences in the spectra between the two groups. However, it is difficult to discriminate details of each component of the saliva samples, such as the mixed ratio of each component. This is because saliva contains too many components to distinguish the intrinsic spectra derived for each independent material. The detailed contents of the saliva cannot be clearly assessed by FT-IR analysis. Regardless, the IR spectra of saliva samples are capable of diagnosing periodontal disease.

Putative explanation for misclassified IR spectra

Most of the samples of periodontal disease could be distinguished based on the differences in the IR spectrum. However, some samples could not be distinguished because individual variations in the distribution of each sample were large. On comparing the log₂-signal values (Fig. 3), the signal from sample S of periodontal disease was lower than those of the other periodontal disease samples. Sample S was obtained from a patient clinically diagnosed with early-lesion periodontal disease (Table 1). Therefore, we believe that the quantities of the saliva contents in sample S were only slightly different from those of the control samples, making the signal value similar to those of the control samples. On the contrary, the signals of control samples G, H, and I were larger than those of the other control samples. Therefore, it is likely these three samples indicate periodontal disease.

The results of the hierarchical cluster analysis by normalized second derivatives classified samples S and Q as controls (Fig. 4). Of the second derivative spectra, the spectrum of sample S, especially in the range of 1300–1000 cm⁻¹, was similar to those of the control samples. As mentioned earlier, sample S also had a low signal value (Fig. 3), and it belonged to a patient clinically diagnosed with early-lesion periodontal disease (Table 1). Therefore, the spectrum of sample S, that is,

the mixture ratio of its components, was similar to those of the control samples.

The observations in case of sample Q were particularly interesting. Sample Q was obtained from a patient clinically diagnosed with an established periodontal lesion (Table 1); furthermore, the signal value for sample Q was relatively high (Fig. 3). The high signal value implied that large quantities of the chemical components were present in the saliva. However, interestingly enough, the shape of the normalized second derivatives of sample Q was similar to those of the controls (Fig. 4); in other words, the mixture ratio of the various components of saliva sample Q was similar to that of control saliva. This unusual finding might indicate another origin for periodontal disease. For example, indigenous bacterium in the oral cavity could cause increased bleeding and gingival inflammation. However, we cannot eliminate the possibility that sample Q may just have been a low-density sample because of a sampling error or individual variation. Although the participants were carefully instructed to follow a particular protocol for providing saliva samples, they may not have followed the protocol properly in some cases. In addition, sample Q could also belong to a person with inherently high moisture content in the oral cavity. These individual variations might be influenced by factors such as age, gender, eating habits, and smoking status.

Samples H and I were derived from control samples, but showed unusually high signal values (Fig. 3). However, the shapes of the normalized second derivatives were similar to those of the control samples (Fig. 4). This situation is similar to that of sample Q. It is difficult to determine the reason for the unusual findings in the case of these two samples. To determine the reasons, we need to collect more samples with detailed individual information, including not only dental diagnosis but also behavioral habits.

Diagnosis by PLS-DA

Finally, supervised classification was carried out using PLS-DA. The contribution of the spectral region between 1700 and 1600 cm^{-1} derived from amide I, which is a protein, appeared to be large (Fig. 5B). This indicated that the quantitative differences in the protein components of saliva affected PLS classification. The predicted values \hat{Y} of the periodontal disease samples were clearly larger than those of the control samples. The accuracy of classification by LOOCV was very high (94.3%). Most of the misclassified spectra were attributed to samples H and S; thus, approximately 30% of the spectra were not diagnosed correctly. The character of the spectra of these samples was different from what was expected of the control samples, and therefore, it is difficult to determine an absolute classification for them.

Nevertheless, it is thought that this methodology, involving FT-IR analysis and PLS-DA discrimination, is very efficient for the diagnosis of periodontal disease. However, the low number of samples analyzed in this study is certainly a limitation because these samples do not represent the different types of periodontal diseases with different etiologies. If the shape of the spectrum that corresponded to a certain diagnosis could be specified and the relevant type of information be accumulated, the method described in this study could be used for determining the causative factors of periodontal disease; moreover, it could be applied to several types of periodontal diseases or even other oral diseases.

Potential for diagnosis by using infrared spectroscopy

Our method involved analyzing the saliva samples and its

constituent complex factors as a whole by FT-IR and using the findings to diagnose periodontal disease. Periodontal diseases have complex etiologies. Our method does not target specific molecules or components of the saliva samples—it assesses all the contents of the saliva. This is because a precise diagnosis can be reached based on the differences in the quantities of the contents of the saliva. However, when unusual spectral findings were obtained, it was difficult to determine their cause. Another methodology or a dentist's diagnosis would be required to elucidate the reason for this unusual finding.

Xiang and co-workers differentiated periodontitis and gingivitis with high accuracy (93.1%) by analyzing the GCF using mid-infrared spectroscopy.²⁶ Their success might be explained by the fact that the GCF contains products directly related to periodontal disease, such as products and enzymes of the causative bacteria. Using our system, we were able to diagnose periodontal disease with high accuracy by analyzing saliva samples with FT-IR microscopy. Our result is interesting because saliva samples contain not only the GCF, but also bacteria from other oral regions such as the tongue coat.

Conclusions

In this study, we established a protocol to collect saliva samples from patients with periodontal disease and healthy volunteers and to perform FT-IR spectroscopy for these samples. The obtained FT-IR spectra contained information about chemical structures, which might be related to the periodontal disease. PLS-DA, a multiple classification analysis, was utilized for discriminating between patients with periodontal disease and healthy volunteers. Using this protocol, we succeeded in diagnosing periodontal disease from saliva samples, with high precision. Further improved classification of periodontal disease should be achieved by applying our protocol to a larger number of samples. Our study suggests the possibility that our method might prove useful for differential diagnosis of diseases of the oral cavity or other diseases if the oral environment is different in these diseases.

Acknowledgements

This work was supported in part by Grants-in-Aid from the Adaptable and Seamless Technology Transfer Program (241FT0492) of the Center for Revitalization Promotion, Japan Science and Technology Agency.

References

1. D. Wolf and I. Lamster, *Dent. Clin. North Am.*, **2011**, *55*, 47.
2. M. Yoshida, *J. Health Care Dent.*, **2005**, *7*, 4.
3. G. C. Armitage, *J. Periodontol.*, **2003**, *74*, 1237.
4. D. Naumann, "Encyclopedia of Analytical Chemistry", ed. R. A. Meyers, **2000**, John Wiley & Sons, Chichester, 102.
5. D. Helm, H. Labischinski, G. Schallehn, and D. Naumann, *J. Gen. Microbiol.*, **1991**, *137*, 60.
6. C. A. Rebuffo-Scheer, C. Kirschner, M. Staemmler, and D. Naumann, *J. Microbiol. Methods*, **2007**, *68*, 282.
7. A. Oust, T. Møretrø, C. Kirschner, J. A. Narvhus, and A. Kohler, *J. Microbiol. Methods*, **2004**, *59*, 149.
8. H. C. Van der Mei, D. Naumann, and H. J. Busscher, *Arch. Oral Biol.*, **1993**, *38*, 1013.

9. E. M. Timmins, S. A. Howell, B. K. Alsberg, W. C. Noble, and R. Goodacre, *J. Clin. Microbiol.*, **1998**, *36*, 367.
 10. A. Bosch, A. Miñán, C. Vescina, J. Degrossi, B. Gatti, P. Montanaro, M. Messina, M. Franco, C. Vay, J. Schmitt, D. Naumann, and O. Yantorno, *J. Clin. Microbiol.*, **2008**, *46*, 2535.
 11. J. J. Ojeda, M. E. Romero-González, and S. A. Banwart, *Anal. Chem.*, **2009**, *81*, 6467.
 12. A. Beljebbar, N. Amharref, A. Lévèques, S. Dukic, L. Venteo, L. Schneider, M. Pluot, and M. Manfait, *Anal. Chem.*, **2008**, *80*, 8406.
 13. T. J. Harvey, A. Henderson, E. Gazi, N. W. Clarke, M. Brown, E. C. Faria, R. D. Snook, and P. Gardner, *Analyst*, **2007**, *132*, 292.
 14. M. Mitsunaga, M. Ogawa, N. Kosaka, L. T. Rosenblum, P. L. Choyke, and H. Kobayashi, *Nat. Med.*, **2011**, *17*, 1685.
 15. S. E. Holton, M. J. Walsh, A. Kajdacsy-Balla, and R. Bhargava, *Biophys. J.*, **2011**, *101*, 1513.
 16. B. Bird, M. S. Miljković, S. Remiszewski, A. Akalin, M. Kon, and M. Diem, *Lab. Invest.*, **2012**, *92*, 1358.
 17. H. Fabian, M. Jackson, L. Murphy, P. H. Watson, I. Fichtner, and H. H. Mantsch Fabian, *Biospectroscopy*, **1995**, *1*, 37.
 18. C. Petibois and G. Déléris, *Trends Biotechnol.*, **2006**, *24*, 455.
 19. K. Z. Liu, C. P. Schultz, R. M. Mohammad, A. M. Al-Katib, J. B. Johnston, and H. H. Mantsch, *Cancer Let.*, **1998**, *127*, 185.
 20. C. P. Schultz, K. Liu, J. B. Johnston, and H. H. Mantsch, *Leuk. Res.*, **1996**, *20*, 649.
 21. J. Kneipp, M. Beekes, P. Lasch, and D. Naumann, *J. Neurosci.*, **2002**, *22*, 2989.
 22. J. Kneipp, P. Lasch, E. Baldauf, M. Beekes, and D. Naumann, *Biochim. Biophys. Acta*, **2000**, *1501*, 189.
 23. J. Schmitt, M. Beekes, A. Brauer, T. Udelhoven, P. Lasch, and D. Naumann, *Anal. Chem.*, **2002**, *74*, 3865.
 24. D. C. Fernandez, R. Bhargava, S. M. Hewitt, and I. W. Levin, *Nat. Biotechnol.*, **2005**, *23*, 469.
 25. B. Bird, M. Miljkovic, M. J. Romeo, J. Smith, N. Stone, M. W. George, and M. Diem, *BMC Clin. Pathol.*, **2008**, *8*, 8.
 26. X. M. Xiang, K. Z. Liu, A. Man, E. Ghiabi, A. Cholakis, and D. A. Scott, *J. Periodontal Res.*, **2010**, *45*, 345.
 27. L. M. Sreebny, *Int. Dent. J.*, **1992**, *42*, 287.
 28. E. Kaufman and I. B. Lamster, *J. Clin. Periodontol.*, **2000**, *27*, 453.
 29. RDC Team R Foundation for Statistical Computing, Vienna, **2006**.
 30. C. A. Lieber and A. Mahadevan-Jansen, *Appl. Spectrosc.*, **2003**, *57*, 1363.
 31. T. Udelhoven, D. Naumann, and J. Schmitt, *Appl. Spectrosc.*, **2000**, *54*, 1471.
 32. P. Lasch, W. Haensch, and E. Lewis, *Appl. Spectrosc.*, **2002**, *56*, 1.
 33. B. H. Mevik and R. J. Wehrens, *J. Statist. Soft.*, **2007**, *18*, 1.
 34. S. De Jong and C. J. F. Ter Braak, *J. Chemom.*, **1994**, *8*, 169.
 35. B. S. Dayal and J. F. MacGregor, *J. Chemom.*, **1997**, *11*, 73.
 36. H. Kurata, S. Awano, A. Yoshida, T. Ansai, and T. Takehara, *J. Med. Microbiol.*, **2008**, *57*, 636.
 37. S. S. Socransky and A. D. Haffajee, *Periodontol 2000*, **2005**, *38*, 135.
 38. B. Paster, S. Boches, and J. Galvin, *J. Bacteriol.*, **2001**, *183*, 3770.
-